



Title	Bulk material based thermoelectric energy harvesting for wireless sensor applications
Author(s)	Wang, Wensi S.; Magnin, Wassim; Wang, Ningning; Hayes, Michael; O'Flynn, Brendan; Ó Mathúna, S. Cian
Publication date	2011
Original citation	Wang, Wensi S.; Magnin, Wassim; Wang, Ningning; Hayes, Michael; O'Flynn, Brendan; Ó Mathúna, S. Cian (2011) 'Bulk material based thermoelectric energy harvesting for wireless sensor applications'. Journal of Physics: Conference Series, 307 (1) 012030. doi: 10.1088/1742-6596/307/1/012030
Type of publication	Article (peer-reviewed)
Link to publisher's version	http://dx.doi.org/10.1088/1742-6596/307/1/012030 Access to the full text of the published version may require a subscription.
Rights	© 2011, The authors. Published under licence in Journal of Physics: Conference Series by IOP Publishing Ltd.
Item downloaded from	http://hdl.handle.net/10468/556

Downloaded on 2017-02-12T07:13:58Z

Bulk Material Based Thermoelectric Energy Harvesting for Wireless Sensor Applications

W S Wang, W Magnin, N Wang, M Hayes, B O'Flynn and C O'Mathuna

Tyndall National Institute, Dyke Parade, Cork, Ireland

E-mail: wensi.wang@tyndall.ie

Abstract. The trend towards smart building and modern manufacturing demands ubiquitous sensing in the foreseeable future. Self-powered Wireless sensor networks (WSNs) are essential for such applications. This paper describes bulk material based thermoelectric generator (TEG) design and implementation for WSN. A 20cm^2 $\text{Bi}_{0.5}\text{Sb}_{1.5}\text{Te}_3$ based TEG was created with optimized configuration and generates 2.7mW in typical condition. A novel load matching method is used to maximize the power output. The implemented power management module delivers $651\mu\text{W}$ to WSN in 50°C . With average power consumption of Tyndall WSN measured at $72\mu\text{W}$, feasibility of utilizing bulk material TEG to power WSN is demonstrated.

1. Introduction

While wireless sensor networks (WSN) have found and created various new applications in recent years, the fundamental problem of short lifetime remains unsolved. New breakthroughs in ultra-low power circuits have reduced the power consumption of wireless sensor modules from mW to the μW level in the last 10 years. Novel network protocols with focus on low power operation further enhance the trend. However, despite of the efforts, coin-sized high energy density lithium batteries can only supply an average load of $100\mu\text{W}$ for less than a year [1]. One simple way to obtain longer lifetime is to use larger or multiple batteries. Although this may extend the lifetime in some cases, it is not commonly acceptable for many applications, especially for wearable and medical wireless sensor networks. Even for applications with little dimension requirement the inevitable battery replacement always brings unfavourable costs and maintenance efforts to the end users.

Harvesting environmental energy is often an effective approach to prolong the battery lifetime or eliminate the battery from the system. Common energy sources can be harvested in daily environment includes heat, light and vibration energy. The thermal energy can be found and used in various locations and conditions. Using thermoelectric energy harvesting to power WSN with aerospace sensors is demonstrated by EADS in [2]. A wrist watch formed thermoelectric generator (TEG) shows ultra-low power wireless communication module powered from human body heat [3]. In the design of TEGs, it has been discovered that the energy conversion efficiency in thermoelectric module and conditioning circuits both play essential roles. The voltage generated from TEG is inherently low due to the limited Seebeck coefficient of materials. With 1 Kelvin temperature difference applied on two sides of one commercial off-the-shelf Bismuth Telluride thermopile, less than 1mV is measured. A MIT team presents a design [4] with 35mV start-up voltage to allow the ultra-low voltage energy harvested with comparatively high efficiency. A similar work is presented by Carlson et al. in [5]. Both of the power management devices require comprehensive and high cost ASIC designs.

In this paper, a different approach is presented. With a simple but essential investigation on bulk material based TEG module, the design is optimized to allow higher voltage output compares to most Peltier cooler modules. A charge pump and switching regulator based power management circuit obtains a start up voltage at 300mV, delivers 650 μ W power. Electric double layer capacitor energy storage is implemented to replace the battery element. A first prototype is demonstrated in section 4. The prototype evaluation was conducted on Tyndall WSN module with integrated temperature and vibration sensing capabilities. The proposed thermal energy powered WSN module can be used to monitor temperature and other parameters in industry and office environment when a 50 degree Celsius temperature is available.

2. Tyndall Wireless Sensor Networks

2.1. Tyndall 25mm Wireless Sensor Module

The Tyndall wireless sensor module is a miniaturized, low-cost multi-function solution for wireless sensing applications. The core of the node is an ATMEL ATmega1281 microcontroller with an 8MHz external crystal oscillator. The ATmega1281 provides eight Analogue-to-Digital Converters (ADC), an Inter-Integrated Circuit bus (I^2C) and eight interrupt pins. This WSN module integrates EM2420 radio chip from EMBER which is 2.4 GHz IEEE 802.15.4 compliant RF transceiver. It interfaced to the microcontroller with a 10 pins bus including a Serial Programmable Interface (SPI).

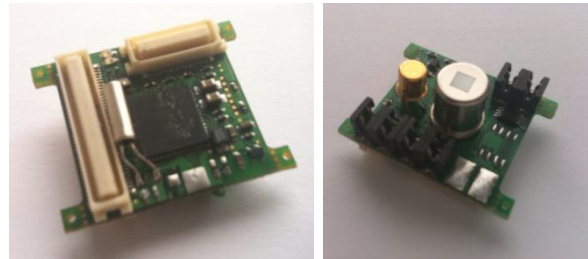
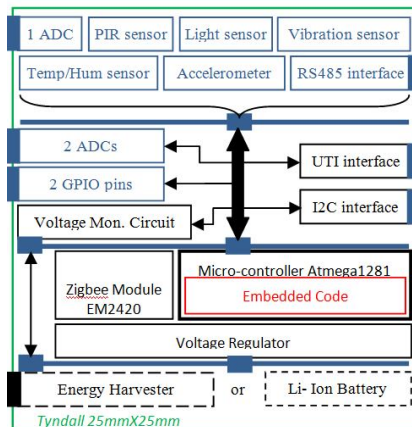


Figure 1. From Left to right: 1) Tyndall 25mm Mote Block Diagram; 2) Micro-Controller and RF Module; 3) Sensor Layer Implementation.

The sensor board is a fully miniaturized integrated sensors layer designated for WSNs. It includes a motion sensor for low-g vibration measurement, a passive infrared sensor (PIR), a light sensor, a 3-axis accelerometer and a temperature-humidity sensor. The accelerometer and temperature-humidity sensors are two digital sensors communicating with I^2C bus. The Tyndall Mote is C programmable. It is also compatible with the TinyOS operation system and the BLIP (Berkeley Low Power IP) stack which is an IP-based protocol implementation. TinyOS drivers have been developed for all the sensors and systems described in figure 1, providing useful libraries of simple software interfaces for embedded network applications development. In order to minimize the embedded code complexity, sensor drivers provide unprocessed data only.

2.2. Power Consumption

The wireless sensor modules operate in duty cycle manner to reach monitoring frequency requirement while conserve the energy by entering low power mode. In every service cycle T_{SP} , the sensing and transmission mode only take place once. The energy consumption in sensing and transmission mode and sleep mode is expressed in Equation 1.

$$E_{Total} = E_{Sleep} + E_{ST} = E_{DTx} + E_{ARx} + E_{Init} + E_{Sen} \quad (1)$$

Where E_{Sleep} and E_{ST} are the energy consumptions in sleep mode and sensing-transmission mode. $E_{\text{DTx}} = 4.6\text{mJ}$, $E_{\text{ARx}} = 0.06\text{mJ}$, $E_{\text{Init}} = 0.4\text{mJ}$ and $E_{\text{Sen}} = 0.4\text{mJ}$ are the data transmission, acknowledgment receiving, board initialization and sensing energy consumptions, respectively. The measurement is taken on Tyndall mote with temperature/humidity sensor and Analog Devices 3-axis accelerometer activated. Both of the sensors require short warm up time, enables an ultra-low duty cycle operation. The detailed energy consumption measurement is presented in Table 1.

Table 1. Energy Consumption Measurement

	Energy(mJ)	Power(mW)	Time(ms)
Sensing and Transmission (ST)	5.46	85.98	63.5
Data Transmission	4.6	131.4	35
Data Receiving	6.1	174.3	35
Mote Initialization	0.4	20	20
Sensing	0.4	53.3	7.5
Acknowledge Transmission	0.05	111.1	0.45
Acknowledge Receiving	0.06	133.3	0.45
Sleep	3.23	0.054	59,847

The time interval between each measurement is one minute in this case. The duty cycle of the operation is measured at 0.1%. The average power consumption is $72\mu\text{W}$ in this typical test condition.

3. Thermoelectric Energy Harvesting

3.1. Thermoelectric Materials

To design a practical thermoelectric energy harvester, several types of thermoelectric materials are investigated for optimized energy conversion rate. The efficiency of a TEG is determined by the dimensionless figure of merit, ZT , The correlation between thermoelectric energy conversion efficiency and ZT figure of merit is shown in Equation 2:

$$\eta = \frac{\Delta T}{T_H} \frac{\sqrt{1+ZT}-1}{\sqrt{1+ZT}+\frac{T_C}{T_H}} \quad (2)$$

A typical cost efficient with relatively high energy conversion efficiency bulk material features a ZT around 0.50-0.75 when located in 300K temperature condition. This was achieved by $\text{Bi}_2\text{Sb}_{2-x}\text{Te}_3$ p-type material in 1960s. A typical TEG implementation based on bulk material is shown in Figure 2.

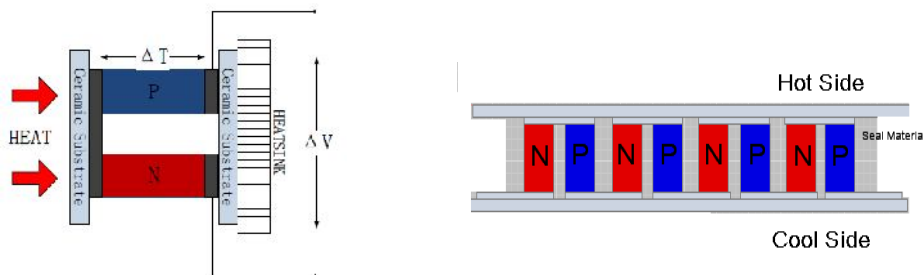


Figure 2. Thermoelectric Module based on Bulk Material

Recent breakthroughs in nano-technology based thermoelectric materials have demonstrated great advantages for ZT improvement. Phonon-blocking superlattices structure material shows the highest ZT figure of merit at 2.4 [6]. These advances certainly show the possibility of high efficiency energy conversion in future TEGs. However, ZT is not the only parameter should be considered when design a TEG. The actual output voltage is a key parameter in TEG design, shown in equation 3. Where α is Seebeck coefficient, N is the number of thermopile pairs, ΔT is the temperature difference between the outer surfaces of two substrates, k and k_C are the thermal conductivities of thermopile and substrate. L and L_C are the thickness of thermopile and substrate.

$$V_o = \frac{\alpha N \Delta T}{1 + 2 \frac{L_C}{L} \frac{k}{k_C}} \quad (3)$$

With the nano material used in TEG, the thickness of thermopiles L will decrease significantly, while the substrate thickness L_C remains the same as in bulk material based design. This effect may substantially reduce the output voltage on single thermopile. Although high number of thermopiles N will be available in nano technology based TEG design. The inevitable high internal resistance makes it impossible to directly utilize the energy without load matching and other power management. The complexity and associated high cost lead to the decision of using bulk material based thermoelectric materials. In this work, $\text{Bi}_{0.5}\text{Sb}_{1.5}\text{Te}_3$ based thermoelectric material with a ZT at 0.7 is used to design thermoelectric modules.

3.2. Thermoelectric Module Design

Thermoelectric module shows behaviors similar to a typical current controlled voltage source when various temperatures applied across it. Similar to other practical voltage source, internal resistance also exists in TEG. To deliver the maximum power output to the load, impedance matching is important. However, different from conventional load matching with fixed internal resistance, in this case the TEG can be modified with different configurations of thermopiles. This leads to a configurable internal resistance. 2 mm^3 sized P type and N type $\text{Bi}_{0.5}\text{Sb}_{1.5}\text{Te}_3$ thermoelectric cubes are used as the basic units of the TEG. With a series connecting configuration, the output power of the TEG can be derived from equation 3. The output power P_{out} is presented in the following equation.

$$P_{out} = \frac{(\alpha N \Delta T)^2 \cdot R_L}{[(1 + 2 \frac{k}{L} \frac{L_C}{k_C}) \cdot (N \cdot R_{TEG} + R_L)]^2} \quad (4)$$

Where R_L is the load resistance and R_{TEG} is the internal resistance of single thermopile, N is the number of series connected thermopiles. The internal resistance of a pair of 2 mm^3 thermopiles is measured at 0.396Ω , while the load resistance in the supercapacitor is 30Ω when operate in low frequency. Without forced convection cooling, the temperature difference between thermopiles only measured at less than 5 Kelvin when 50 degree Celsius is applied on high temperature side. Due to the small form factor nature of the WSN, the size of the TEG should no larger than 60mm by 60mm. This factor limits the number of thermopiles pairs to less than 200. A simulation is conducted with above predetermined conditions. The output power to the supercapacitor is presented in the following figure.

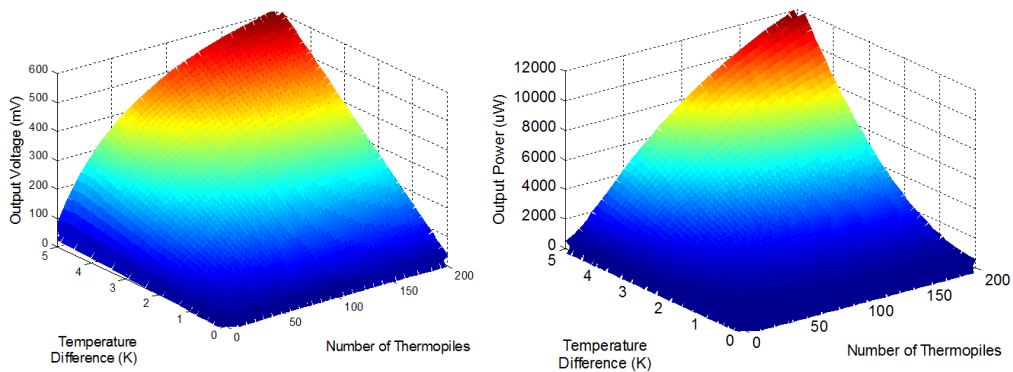


Figure 3. Output Voltage and Output Power Analysis

The temperature difference shown in this figure is the temperature difference on the two ceramic substrates, instead on the thermopiles directly. The simulation results illustrated in figure 3 show the required $72 \mu\text{W}$ can be obtained from the TEG when 36 thermopiles connected in series at one Kelvin temperature difference. However, under the same condition, the output voltage on the supercapacitor is only 52.4mV. To operate without ASIC based DC/DC conversion circuit, the minimum voltage output should be higher than 300mV. In the worst case scenario, when the temperature on the hot side is 50 degree Celsius, the temperature difference on the substrates is 3.5 Kelvin when minimum airflow

is measured in laboratory condition. In this case, to obtain a 300mV output voltage, the minimum number of thermopile is 120. With this number of thermopiles integrated in the TEG, the output power is 2.96mW. Based on this analysis, a 16 by 16 thermopile legs (P/N type cubes) array is created, given a thermopile number at 128. The device is measured at 45mm by 45mm.

3.3. Power Management

In this implementation, low cost off-the-shelf components are utilized to step up the output voltage of TEG to usable voltage for WSN. A Texas Instruments TPS61200 boost converter and a Seiko Instruments S-882Z18 charge pump are selected due to their high efficiency in ultra-low voltage conditions. To step up the output voltage from 300mV, directly utilizing a boost converter is not feasible since the starting voltage of boost converter is substantially higher. The power management circuit is shown in Figure 4.

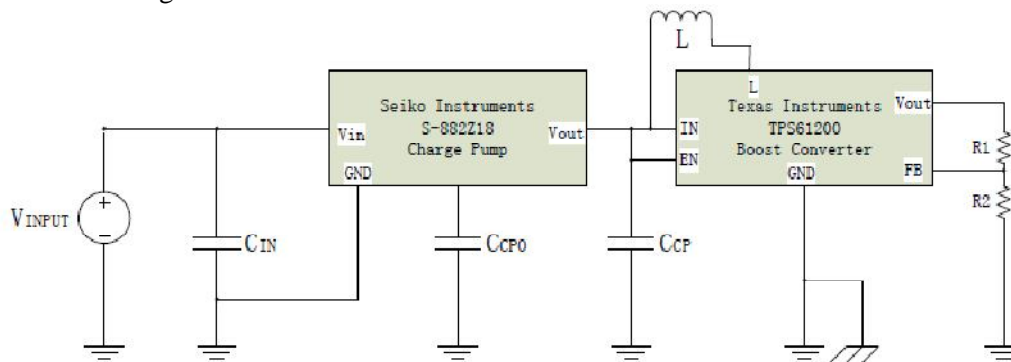


Figure 4. Simplified Step-up DC/DC Conversion

The ultra-low input voltage of Seiko Instruments S-882Z enables a start up voltage at 300mV. Once the voltage of TEG boosts to above the threshold, the voltage on the output capacitor of the charge pump increases until it reaches the start up voltage of the boost converter at 700mV. The Enable pin is controlled manually in this case to assist the start up process. It also can be connected to a comparator based self start controller similar to a design presented in previous work [1]. It employs a MAX931 ultra-low power comparator to detect the V_{CCP} until it settled at the 700mV and enabled the DC/DC converter to step up to 3.3V.

4. Thermoelectric Generator Powered WSN Implementation

Based on the proposed TEG design, the assembling and packaging was conducted by [6]. Due to the fact WSN operates in duty cycling manner, energy buffer is essential to avoid periodic power failure. Electric double-layer capacitor (supercapacitor) is the selected energy storage in this work. Low equivalent series resistance (ESR) energy storage unit is used to avoid sudden voltage drop in the WSN active mode. While high density type supercapacitor is connected in parallel to increase the capacity. Additionally, energy failure detection circuit is integrated using a voltage comparator to detect low voltage condition in supercapacitor. The failure detection is based on Seiko Instruments S-89530A ultra-low power (5 pA) comparator. The prototype is shown in Figure 5.

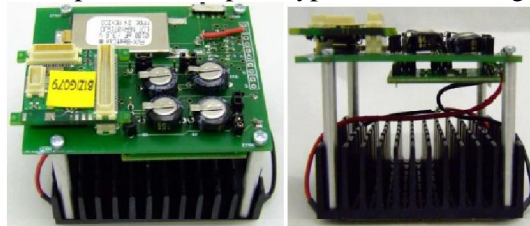


Figure 5. Thermoelectric Powered WSN Prototype

The viability of the TEG design and the application on WSN were tested through a set of experiments. The prototype was placed on hotplate in various temperatures to test the start up performance, continuous operation and finally energy storage lifetime when no thermal energy is available.

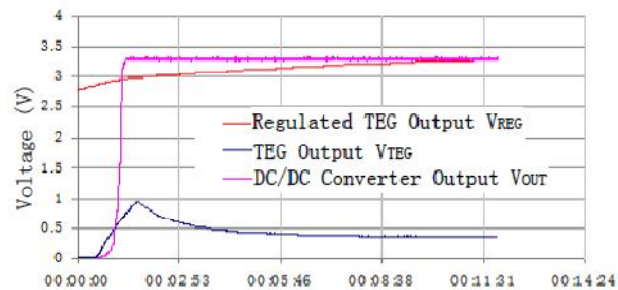


Figure 6. TEG Start-up Performance

The above figure shows the start up performance when prototype deployed on 50 degree Celsius temperature. The initial elevated temperature difference was clearly observed when output voltage peaked at 1 minute 25 second from the beginning of the test at 0.97V. This effect automatically starts up the boost converter. The switching regulator operates in continuous mode providing a stable output at 3.3V to the WSN when output voltage of TEG drop back to 350mV in the later stage of start up. The supercapacitor was pre-charged to 2.7V in this experiment. The charging lasts 11 minutes and 30 seconds to reach 97% of the full charge. The TEG obtains an output power at 2.7mW, which consistent with the simulation results with an 8.7% error. The power management circuit features average conversion efficiency at 55%. The leakage current on the supercapacitor and the output end power conversion further decreases the conversion efficiency. The available power delivered from TEG to WSN is measured at 651 μ W.

5. Conclusions

A thermoelectric powered wireless sensor module which eliminates the need for a battery is developed. The relative simplicity of the design and utilizing bulk material thermopiles plays a major role in reducing the system cost. The verified implementation, with Bi_{0.5}Sb_{1.5}Te₃ based thermopiles arranged in a 16 by 16 configuration deliver 2.7mW when 50 degree Celsius temperature is applied upon. The power management features a charge pump and switching regulator design. It steps up the voltage from 300mV to 3.3V. The power delivered to WSN is measured at 651 μ W in this typical condition. The generated power is substantially higher than the average power consumption of WSN at 72 μ W. The results demonstrated the feasibility of using bulk material based TEG to achieve power autonomous in many WSN applications.

Acknowledgments

This work has been funded by Scientific Foundation Ireland through ITOBO (398-CRP) project and EU FP-7 through Nanofunction (257375) project.

References

- [1] Wang W S, O'Donnell T, Wang N, Hayes M, O'Flynn B and O'Mathuna C 2010 *J. Emerg. Technol. Comput. Syst.* **6** 1-26
- [2] Becker T, Kluge M, Schalk J, Tiplady K, Paget C, Hilleringmann U and Otterpohl T 2009 *Sensors. J.* **9** 1589-95
- [3] Leonov V, Torfs T, Fiorini P and Van Hoof C 2007 *Sensors. J* **7** 650-57
- [4] Ramadass Y K and Chandrakasan A P 2011 *Solid-State Circuits* **46** 333-41
- [5] Carlson E, Strunz K and Otis B P 2010 *Solid-State Circuits* **45** 741-50
- [6] Venkatasubramanian R, Siivola E, Colpitts T and O'Quinn B 2001 *Nature* **413** 597-602.
- [7] Thermonamic: <http://www.thermonamic.com/>